Experimental topological photonic superlattice

Yao Wang, Yong-Heng Lu, Jun Gao, Yi-Jun Chang, Hao Tang, and Xian-Min Jin*

Center for Integrated Quantum Information Technologies (IQIT), School of Physics and Astronomy and State Key Laboratory of Advanced Optical Communication Systems and Networks, Shanghai Jiao Tong University, Shanghai 200240, China and

CAS Center for Excellence and Synergetic Innovation Center in Quantum Information and Quantum Physics, University of Science and Technology of China, Hefei, Anhui 230026, China

(Received 27 August 2019; accepted 25 November 2020; published 15 January 2021)

Topological phase, possessing inherent robustness against disorder, plays a central role in understanding matter, tailoring properties of artificial materials, and holding the promise of fault-tolerant quantum simulation and computing. Various topological phases and accessible controllability are being enthusiastically pursued in a wide spectrum ranging from condensed-matter to photonic systems. Recently, a topological photonic superlattice with arbitrary number of sites in each unit cell was proposed to provide richer topological properties. Here we successfully map such a multipartite structure into a photonic chip by using a femtosecond laser direct writing technique and demonstrate a direct observation of topological photonic superlattices in the quantum regime. Besides the tunable number of topologically protected edge states, we also observe stable interface states induced by the interference of topological linear modes, which exhibits Bloch-oscillation-like breathing dynamic behavior but free of nonlinearity.

DOI: 10.1103/PhysRevB.103.014110

I. INTRODUCTION

Nontrivial properties of new artificial materials and structures are the pursuits in material science. Topological phase, deriving from the quantum Hall effect, is found to be a new powerful tool and plays a fundamental role in understanding matter [1–5]. In the past decades, topological robust phases have been widely investigated in ultracold-matter [6–8], condensed-matter [2,3], and photonic systems [4,5,9–18]. The extraordinary robustness of the topological phase has found promising applications for inherently fault-tolerant quantum simulation and quantum computing [19].

The Su-Schrieffer-Heeger (SSH) model describing a lattice of dimers is the conceptually simplest system that can possess topological trivial and nontrivial states [20]. In view of band structures, the former one is described by a gapped spectrum while there is a zero-energy edge mode in the middle of the gap for the latter one. These two distinct states can be conveniently tuned by the relative value between the intercell and the intracell coupling strengths. The topological features of the SSH model have been widely observed in experiments [2–5,8,21–27].

For the SSH model [20] and other structures [12], there are fixed and limited numbers of nontrivial phases in the system. Recently, a superlattice beyond the standard SSH model was proposed and richer topological properties were predicted [28]. The most intriguing feature of the superlattice is the multiple topologically nontrivial dispersion bands; furthermore, the number of edge states in the superlattice is tunable. Such a unique feature will allow one flexible control over the topological states in a new domain. An interface-state-induced oscillatory dynamic can arise due to the interference of topological linear modes. Besides the robustness against disorder, the interface state can behave similarly to the Bloch oscillation but without the appearance of nonlinearity.

Compared with other information carriers, a photon is easier to be created and detected, and has been employed to investigate topological phenomena [4,5]. The single photon, as a promising platform for quantum simulation and quantum computing [29–31], is most likely to be simultaneously compatible for both topological physics and quantum information [27,32]. The compatibility of a single photon between topological states and single particles is able to extend the topological protection into the quantum regime, which suggests quantum topological photonics as a new frontier for exploring both fundamental problems and potential applications [33–37]. Therefore, it is highly desirable to realize both the multiple topologically nontrivial state and the interface state in a single-photon level, which may provide an entirely new resource and controllable degree of freedom for future topologically protected quantum networks and quantum information processing.

In this work, we construct a multiband photonic superlattice and successfully observe multiple topological edge states and the interface states via single-photon dynamic. The single photon is strongly localized in a boundary of the fabricated three- and four-sited unit cell superlattice chains. The breathinglike oscillatory dynamic is observed at the interface connecting two superlattices in the trivial and nontrivial phases, respectively. We also demonstrate the interface states, where the periodic feature of the single-photon dynamics is maintained after introducing disorder.

*xianmin.jin@sjtu.edu.cn

 ©2021 American Physical Society

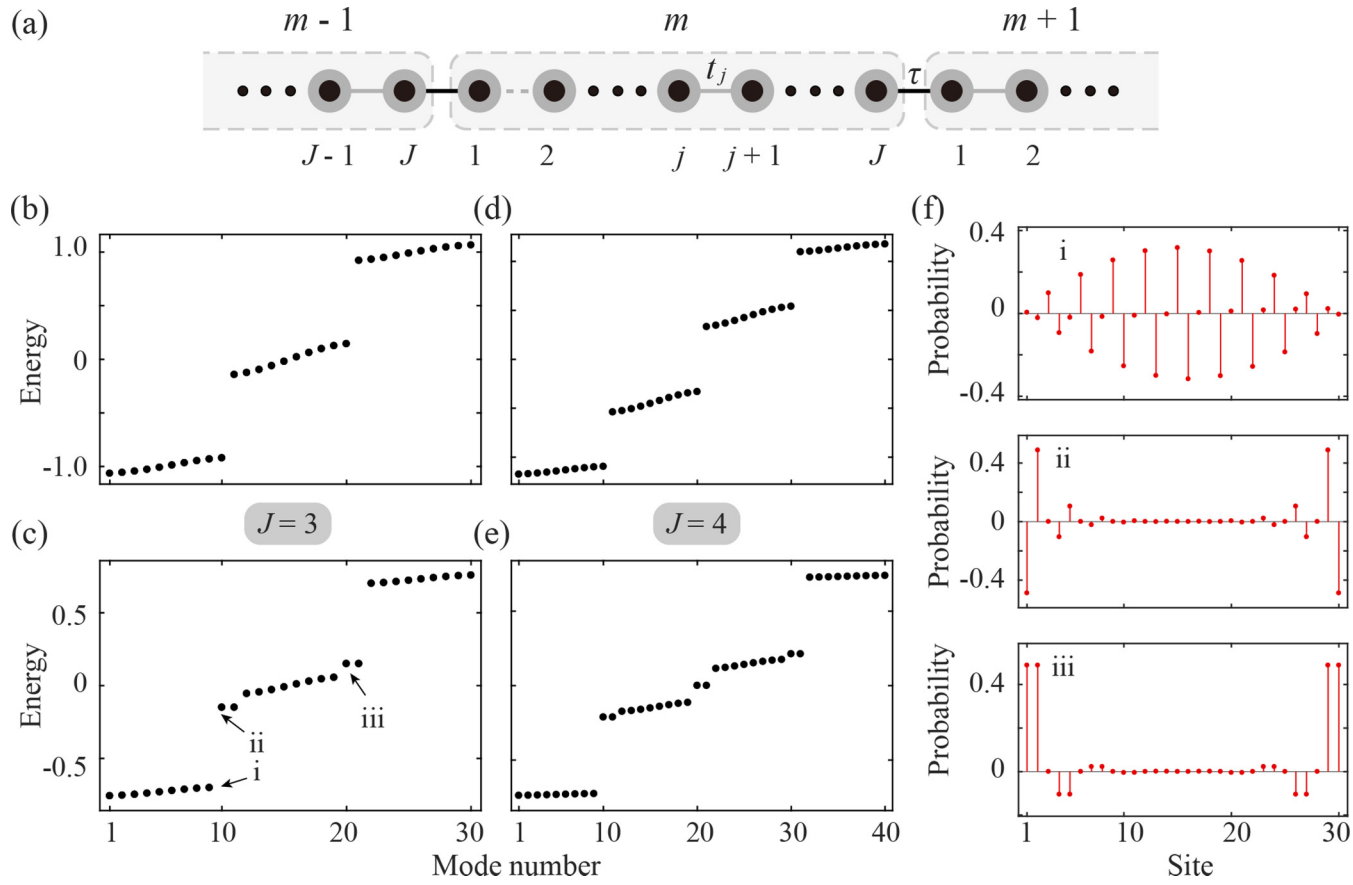

FIG. 1. Structure and spectrum of the superlattice. (a) The schematic of the superlattice. The superlattice with the nearest-neighbor coupling contains M unit cells and J sites in each cell. Therefore, there are $M \times J$ sites in the lattice. (b–e) The eigenspectra of superlattices which contain different site numbers $J = 3$ and $J = 4$. There are $J - 1$ gaps in the band structure, and two edge sates in each gap for the topological nontrivial structure (c, e) but not for the trivial cases (b, d). (f) The spatial distributions of the bulk state and edge states of the superlattice with $J = 3$. The photon is distributed in all the sites for the bulk state (i) but localized in the end of the lattice for the edge state (ii, iii). The parameters are picked as $\tau = 0.7$ and $t = 0.15$ in the calculation.

II. MODEL

As shown in Fig. 1(a), considering a superlattice that contains $M \times J$ sites, where M is the unit cell number and J is the site number in each cell, and only nearest-neighbor coupling exists, the Hamiltonian of the system can be described by

$$H = \sum_{m=1}^{M} \sum_{j=1}^{J-1} t_j a_{m,j}^{+} a_{m,j+1} + \tau a_{m,J}^{+} a_{m+1,1} + \text{H.c.}, \qquad (1)$$

where $a_{m,j}^{+}$ ($a_{m,j}$) is the Bosonic creation (annihilation) operator at site j in the mth unit cell, t_j presents the intracell coupling strength between the adjacent sites j and $j + 1$, and the τ is the intercell coupling strength.

For $j = 1$ and 2, the system reduces to the homogeneous lattices and SSH model, respectively, which have been well studied. It is more interesting for the cases of $J > 2$, where the lattice owns topologically protected multiple edge and interface states. We show the calculated band structure of the photonic superlattice in Figs. 1(b)–1(e) for the cases of $J = 3$ and $J = 4$. The coupling parameters in each unit cell are set to be symmetric with respect to the center site. There are $J - 1$ gaps that separate the energy band. The edge states exist when the intercell coupling τ is larger than the intracell coupling t [see Figs. 1(c) and 1(e)], but not for the inverse case [see Figs. 1(b) and 1(d)].

We further show the spatial distribution of the bulk state and edge states in Fig. 1(f) for the case of $J = 3$. It is defined by $D_n(E) = \sum_m \delta(E - E_m)|\varphi_n^{(m)}|^2$, where E_m is the energy of the mth eigenstate and $\varphi_n^{(m)}$ is its wave function. The single photons distribute over all the sites in the bulk state, as shown in Fig. 1(f-i). In contrast, the single photon is confined on the boundary of lattice under the norm of the edge states as the spatial distribution implied in Figs. 1(f-ii) and 1(f-iii).

III. BOUNDARY STATES

We fabricate the superlattices in borosilicate glass using the femtosecond laser direct writing technique [38–41], which allows us to map a three-dimensional lattice into a photonic chip in a controllable fashion [42]. We set the parameter $M = 10$ and implement two superlattices with $J = 3$ and 4, respectively. Heralded single photons are injected into the leftmost site and the rightmost site to observe the edge states for both lattices, and the outgoing probability distributions are captured by an intensified charge-coupled device (ICCD)

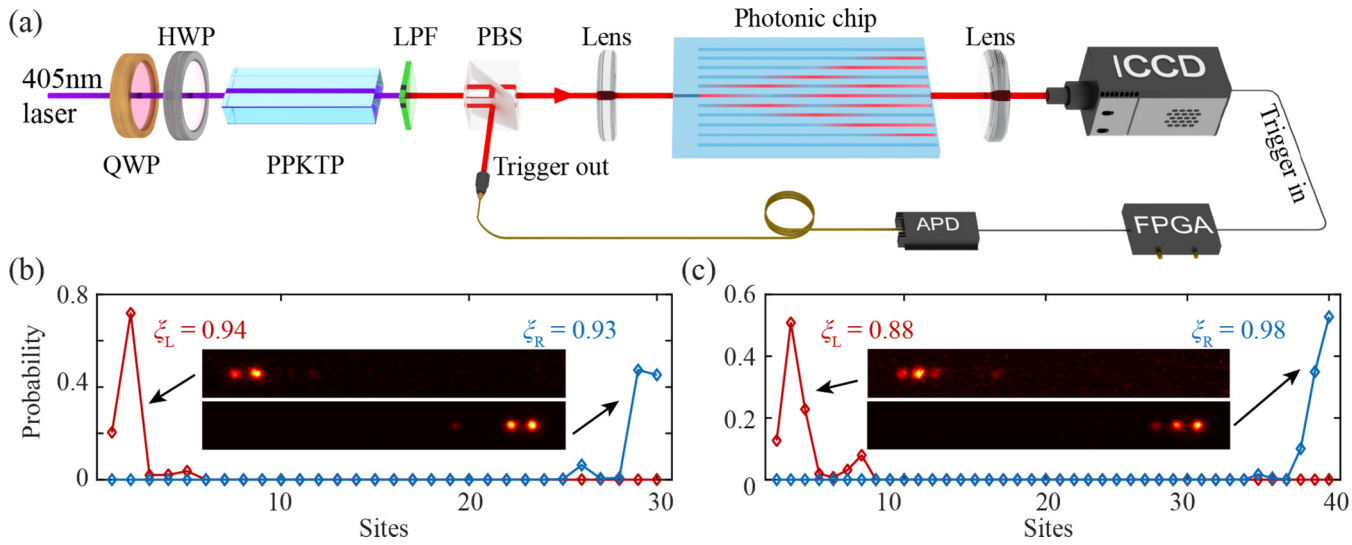

FIG. 2. Experimental observation of edge states for superlattices. (a) The sketch of the experimental setup. Different superlattices are fabricated in the same photonic chip. Heralded single photons generated from the periodically poled potassium titanyl phosphate (PPKTP) crystal are injected into the lattices after being focused by a lens and collected at the output facet by an ICCD after being collimated. (b, c) The measured edge states of superlattices. Both the left (red) and right (blue) edge states of superlattices are observed for (b) $J = 3$ and (c) $J = 4$. The parameters picked in the experiment are the same as those in the simulation.

camera after hopping through 40 mm [see Fig. 2(a) for more details].

The experimental results of the single-photon distribution probability are shown in Figs. 2(b) and 2(c). From the distribution probability at the outgoing facet, one can find that the single photons occupy the sites in the first and last unit cells with high probability, implying the existence of both the left and right edge states. To quantify the localization on the edge, we calculate the generalized return probability $\xi_{L/R}$ of left and right edge states defined by $\xi_{L/R} = \sum_{k-d}^{k+d} I_i / \sum_1^n I_i$, which quantifies the probability of the single photon that remains within a small distance d from the injection site k, and the accumulated distance $d = J$ is the width of the localized boundary state. In our experiment, $\xi_L = 0.94$ and $\xi_R = 0.93$ for the superlattice with $J = 3$, while $\xi_L = 0.88$ and $\xi_R = 0.98$ for the superlattice with $J = 4$, which is a clear signature of the existence of boundary states.

IV. BLOCH-LIKE OSCILLATION DYNAMICS

Because the edge states in different band gaps are all localized at the same spatial sites in our system, all the edge modes are excited in the above experimental implementation. Thus, the observed existence of the edge modes solely cannot demonstrate the multiband feature of the superlattice. Fortunately, another attractive phenomenon about the superlattice could help us to demonstrate the multiband feature: the breathinglike oscillation induced by the interference of

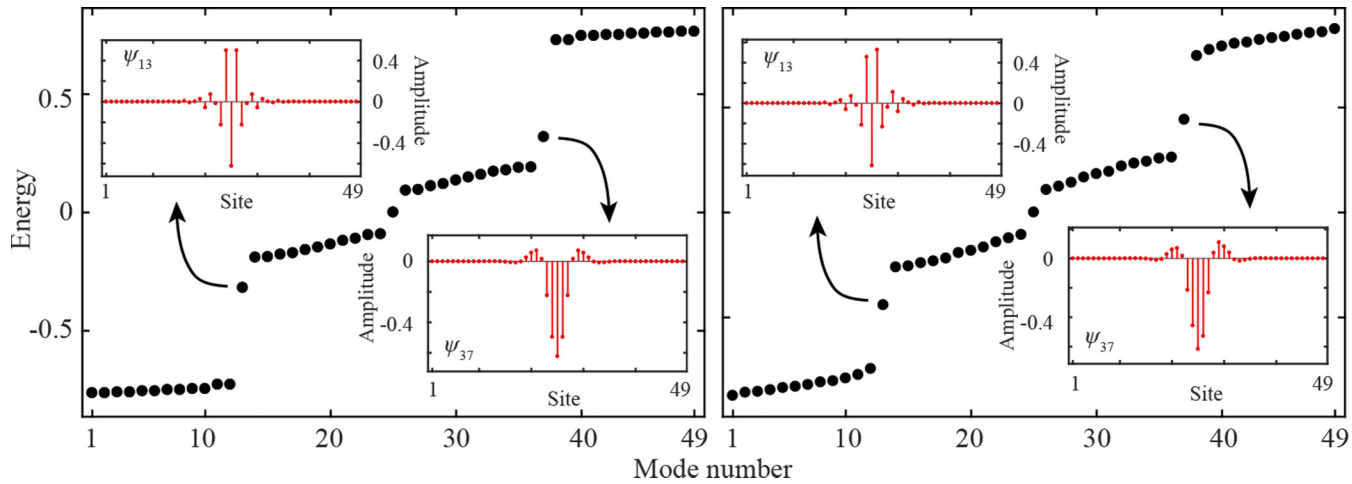

FIG. 3. Topological interface states. The propagation-constant spectrum of superlattices (left) without and (right) with disorder with $J = 4$ shows that there are three interface states in the gap. The band structure and the spatial distributions do not change much even after introducing the disorder. The parameters are picked as $\tau = 0.7$, $t_1 = t_3 = 0.2$, and $t_2 = 0.15$. The disorder is introduced by adding uniformly distributed random coupling strength varying from 0 to 0.1 for each coupling.

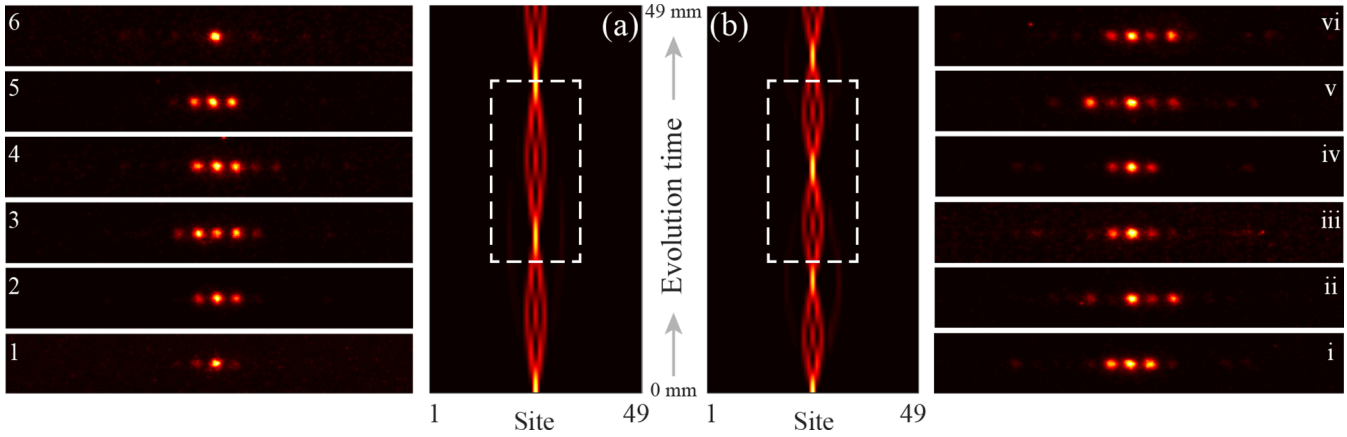

FIG. 4. Direct observation of topological interface states. (a) The interface state forming a breathinglike oscillation owns the similar dynamic with Bloch oscillation. We observe a complete periodical dynamic in the experiment by measuring the output distribution under different evolution distance (1–6) varying from 20 to 45 mm with step size of 5 mm. (b) The stability of interface-state propagation against disorder is well experimentally demonstrated (i–vi). The parameters picked in the experiment are the same as those in the simulation.

topological linear modes of different propagation constants, which does not exist for the case $J < 3$.

To observe the dynamics of such a topological interface state, a convenient way is to construct a lattice which combines two subsuperlattices of different topological phases and excite the lattice from the interface site. We set parameters as $\tau = 0.7$, $t_1 = t_3 = 0.2$, and $t_2 = 0.15$ and show the band structure taking the case $J = 4$ for example in Fig. 3, where three localized edge states exist in the gap. Two spatial distributions of the edge states are shown in the insets, which are the 13th and 37th eigenstates in the band structure. The interference state will appear when the single photon is interfered among the three different topological linear modes.

What is more, we introduce the disorder by adding uniform distributed random coupling strength varying from 0 to 0.1 for each coupling. The band structure and the spatial distributions of the edge states do not change much after introducing the disorder as shown in Fig. 3. The intrinsic interference state promises a practical application in photonic networks and devices for quantum information processing.

To observe and explore the breathing-like interference states dynamics in the experiment, we fabricated six superlattices with different evolution distance varying from 20 to 45 mm with step size of 5 mm. As is shown in Fig. 4(a), the simulated result shows that the heralded single photons are stably oscillated and localized in the interface of two superlattices. The experimental observation, as is shown in the inset (1–6), demonstrates the Bloch-like oscillation induced by the topological interface state. The observed Bloch-like oscillation confirms the multiband feature of the photonic superlattice.

We further introduce random disorder into the structure to experimentally explore the stability of the phenomenon to disorder. The simulated and experimental results are shown in Fig. 4(b). The interference of topological states is found to be very stable. It is worthwhile to mention that the oscillation period shown here is smaller than the lattice without disorder. It is attributed to the fact that the average coupling of the disordered lattice is larger than that of the pure lattice, which is related to the manner of practical disorder realization in our work. In fact, the period of the Bloch-like oscillations is still preserved in the presence of disorder. The detailed discussion on oscillation period can be found in the Supplemental Material [43].

V. CONCLUSION

In conclusion, we demonstrate the appearance of multiple topological edge states of single photons in a superlattice and the performance of an interface-state-induced Bloch-like oscillation dynamic. By using a single-photon imaging technique and the femtosecond laser direct writing technique, we are able to experimentally confirm the compatibility between macroscopic topological states in a superlattice and microscopic single photons on a photonic chip.

Our work represents an attempt to extend the topological phase into the quantum regime, combining topological physics and quantum information. The results presented here show that there are richer topological properties in multiband superlattices and these properties are compatible with the single-photon quantum feature, which may provide an entirely new resource and controllable degree of freedom and pave the way towards fundamental investigation of quantum topological photonics and potential applications on artificial topological devices.

ACKNOWLEDGMENTS

The authors thank Jian-Wei Pan for helpful discussions. This research is supported by the National Key R&D Program of China (Grants No. 2019YFA0706302, No. 2017YFA0303700, and No. 2019YFA0308700), National Natural Science Foundation of China (Grants No. 11904229 No. 11761141014, No. 61734005, and No. 11690033), Science and Technology Commission of Shanghai Municipality (Grants No. 17JC1400403 and No. 2019SHZDZX01), and Shanghai Municipal Education Commission (Grant No. 2017-01-07-00-02-E00049). X.-M.J. acknowledges additional support from a Shanghai talent program and support from Zhiyuan Innovative Research Center of Shanghai Jiao Tong University.

[1] K. von Klitzing, G. Dorda, and M. Pepper, New Method for High-Accuracy Determination of the Fine-Structure Constant Based on Quantized Hall Resistance, Phys. Rev. Lett. **45**, 494 (1980).

[2] M. Z. Hasan and C. L. Charles, Topological insulators, Rev. Mod. Phys. **82**, 3045 (2010).

[3] X. L. Qi and S. C. Zhang, Topological insulators and superconductors, Rev. Mod. Phys. **83**, 1057 (2011).

[4] L. Lu, J. D. Joannopoulos, and M. Soljačić, Topological photonics, Nat. Photonics **8**, 821 (2014).

[5] T. Ozawa, H. M. Price, Al. Amo, N. Goldman, M. Hafezi, L. Lu, M. C. Rechtsman, D. Schuster, J. Simon, O. Zilberberg, and I. Carusotto, Topological photonics, Rev. Mod. Phys. **91**, 015006 (2019).

[6] M. Atala, M. Aidelsburger, J. T. Barreiro, D. Abanin, T. Kitagawa, E. Demler, and I. Bloch, Direct measurement of the Zak phase in topological Bloch bands, Nat. Phys. **9**, 795 (2013).

[7] G. Jotzu, M. Messer, R. Desbuquois, M. Lebrat, T. Uehlinger, D. Greif, and T. Esslinger, Experimental realization of the topological Haldane model with ultracold fermions, Nature **515**, 237 (2014).

[8] D.-W. Zhang, Y.-Q. Zhu, Y. X. Zhao, H. Yan, and S.-L. Zhu, Topological quantum matter with cold atoms, Adv. Phys. **67**, 253 (2018).

[9] F. D. M. Haldane and S. Raghu, Possible Realization of Directional Optical Waveguides in Photonic Crystals with Broken Time-Reversal Symmetry, Phys. Rev. Lett. **100**, 013904 (2008).

[10] D. Hsieh, D. Qian, L. Wray, Y. Xia, Y. S. Hor, R. J. Cava, and M. Z. Hasan, A topological Dirac insulator in a quantum spin Hall phase, Nature **452**, 970 (2008).

[11] Z. Wang, Y. Chong, J. D. Joannopoulos, and M. Soljačić, Observation of unidirectional backscattering-immune topological electromagnetic states, Nature **461**, 772 (2009).

[12] Y. E. Kraus, Y. Lahini, Z. Ringel, M. Verbin, and O. Zilberberg, Topological States and Adiabatic Pumping in Quasicrystals, Phys. Rev. Lett. **109**, 106402 (2012).

[13] M. Hafezi, S. Mittal, J. Fan, A. Migdall, and J. M. Taylor, Imaging topological edge states in silicon photonics, Nat. Photonics **7**, 1001 (2013).

[14] M. C. Rechtsman, Y. Plotnik, J. M. Zeuner, D. Song, Z. Chen, A. Szameit, and M. Segev, Topological Creation and Destruction of Edge States in Photonic Graphene, Phys. Rev. Lett. **111**, 103901 (2013).

[15] M. C. Rechtsman, J. M. Zeuner, Y. Plotnik, Y. Lumer, D. Podolsky, F. Dreisow, S. Nolte, M. Segev, and A. Szameit, Photonic Floquet topological insulators, Nature **496**, 196 (2013).

[16] X. Cheng, C. Jouvaud, X. Ni, S. H. Mousavi, A. Z. Genack, and A. B. Khanikaev, Robust reconfigurable electromagnetic pathways within a photonic topological insulator, Nat. Mater. **15**, 542 (2016).

[17] L. Lu, Z. Wang, D. Ye, L. Ran, L. Fu, J. D. Joannopoulos, and M. Soljačić, Experimental observation of Weyl points, Science **349**, 622 (2015).

[18] J. Noh, S. Huang, D. Leykam, Y. Chong, K. P. Chen, and M. C. Rechtsman, Experimental observation of optical Weyl points and Fermi arcs, Nat. Phys. **13**, 611 (2017).

[19] C. Nayak, S. H. Simon, A. Stern, M Freedman, and S. Das Sarma, Non-Abelian anyons and topological quantum computation, Rev. Mod. Phys. **80**, 1083 (2008)

[20] W. P. Su, J. R. Schrieffer, and A. J. Heeger, Solitons in Polyacetylene, Phys. Rev. Lett. **42**, 1698 (1979).

[21] A. Blanco-Redondo, I. Andonegui, M. J. Collins, G. Harari, Y. Lumer, M. C. Rechtsman, B. J. Eggleton, and M. Segev, Topological Optical Waveguiding in Silicon and the Transition between Topological and Trivial Defect States, Phys. Rev. Lett. **116**, 163901 (2016).

[22] E. J. Meier, F. A. An, and B. Gadway, Observation of the topological soliton state in the Su-Schrieffer-Heeger model, Nat. Commun. **7**, 13986 (2016).

[23] P. St-Jean, V. Goblot, E. Galopin, A. Lemaître, T. Ozawa, L. Le Gratiet, I. Sagnes, J. Bloch, and A. Amo, Lasing in topological edge states of a one-dimensional lattice, Nat. Photonics **11**, 651 (2017).

[24] H. Zhao, P. Miao, M. H. Teimourpour, S. Malzard, R. El-Ganainy, H. Schomerus, and L. Feng, Topological hybrid silicon microlasers, Nat. Commun. **9**, 981 (2018).

[25] M. Parto, S. Wittek, H. Hodaei, G. Harari, M. A. Bandres, J. Ren, M. C. Rechtsman, M. Segev, D. N. Christodoulides, and M. Khajavikhan, Edge-Mode Lasing in 1D Topological Active Arrays, Phys. Rev. Lett. **120**, 113901 (2018).

[26] M. Pan, H. Zhao, P. Miao, S. Longhi, and L. Feng, Photonic zero mode in a non-Hermitian photonic lattice, Nat. Commun. **9**, 1308 (2018).

[27] Y. Wang, Y.-H. Lu, F. Mei, J. Gao, Z.-M. Li, H. Tang, S.-L. Zhu, S. Jia, and X.-M. Jin, Direct Observation of Topology from Single-Photon Dynamics, Phys. Rev. Lett. **122**, 193903 (2019).

[28] B. Midya and L. Feng, Topological multiband photonic superlattices, Phys. Rev. A **98**, 043838 (2018).

[29] A. Aspuru-Guzik and P. Walther, Photonic quantum simulators, Nat. Phys. **8**, 285 (2012).

[30] H. Tang, X. F. Lin, Z. Feng, J. Y. Chen, J. Gao, X. Y. Xu, Y. Wang, L. F. Qiao, A. L. Yang, and X. M. Jin, Experimental two-dimensional quantum walk on a photonic chip, Sci. Adv. **4**, eaat3174 (2018).

[31] H. Tang, C. D. Franco, Z.-Y. Shi, T.-S. He, Z. Feng, J. Gao, K. Sun, Z.-M. Li, Z.-Q. Jiao, T.-Y. Wang, M. S. Kim, and X.-M. Jin, Experimental quantum fast hitting on hexagonal graphs, Nat. Photonics **12**, 754 (2018).

[32] Y. Wang, Y. H. Lu, J. Gao, K. Sun, Z. Q. Jiao, H. Tang, and X. M. Jin, Quantum topological boundary states in quasicrystal, Adv. Mater. **31**, 1905624 (2019).

[33] S. Mittal, E. A. Goldschmidt, and M. Hafezi, A topological source of quantum light, Nature **561**, 502 (2018).

[34] J.-L. Tambasco, G. O. Corrielli, R. J. Chapman, A. Crespi, O. Zilberberg, R. Osellame, and A. Peruzzo, Quantum interference of topological states of light, Sci. Adv. **4**, eaat3187 (2018).

[35] A. Blanco-Redondo, B. Bell, D. Oren, B. J. Eggleton, and M. Segev, Topological protection of biphoton states, Science **362**, 568 (2018)

[36] Y. Wang, X.-L. Pang, Y.-H. Lu, J. Gao, Y.-J. Chang, L. F. Qiao, Z.-Q. Jiao, H. Tang, and X.-M. Jin, Topological protection of two-photon quantum correlation on a photonic chip, Optica **6**, 955 (2019).

[37] Y. Wang, Y.-H. Lu, J. Gao, R.-J. Ren, Y.-J. Chang, Z.-Q. Jiao, Z.-Y. Zhang, and X.-M. Jin, Topological protected quantum entanglement, arXiv:1903.03015.

[38] K. M. Davis, K. Miura, N. Sugimoto, and K. Hirao, Writing waveguides in glass with a femtosecond laser, Opt. Lett. **21**, 1729 (1996).

[39] A. Szameit, F. Dreisow, T. Pertsch, S. Nolte, and A. Tünnermann, Control of directional evanescent coupling in fs laser written waveguides, Opt. Express **15**, 1579 (2007).

[40] A. Crespi, R. Osellame, R. Ramponi, D. J. Brod, E. F. Galvão, N. Spagnolo, C. Vitelli, E. Maiorino, P. Mataloni, and F. Sciarrino, Integrated multimode interferometers with arbitrary designs for photonic boson sampling, Nat. Photonics **7**, 545 (2013).

[41] Z. Chaboyer, T. Meany, L. G. Helt, M. J. Withford, and M. J. Steel, Tunable quantum interference in a 3D integrated circuit, Sci. Rep. **5**, 9601 (2015).

[42] Y. Wang, J. Gao, X. L. Pang, Z. Q. Jiao, H. Tang, Y. Chen, L. F. Qiao, Z. W. Gao, J. P. Dou, A. L. Yang, and X. M. Jin, Parity-Induced Thermalization Gap in Disordered Ring Lattices, Phys. Rev. Lett. **122**, 013903 (2019).

[43] See Supplemental Material at http://link.aps.org/supplemental/10.1103/PhysRevB.103.014110 for the features of the period of the Bloch-like oscillation.